Electric transport coefficients in highly epitaxial LaBaCo2O5 + δ films with "p-to-n" transition induced by...

Article *in* Journal of Applied Physics · August 2016

DOI: 10.1063/1.4960688

6 authors, including:

Jamal Shaibo
Dalian University of Technology
5 PUBLICATIONS **2** CITATIONS
SEE PROFILE

Lujun Pan
Dalian University of Technology
107 PUBLICATIONS **1,377** CITATIONS
SEE PROFILE

AIP Journal of Applied Physics

Electric transport coefficients in highly epitaxial LaBaCo2O5+δ films with "p-to-n" transition induced by oxygen deficiency

J. Shaibo, Q. Y. Zhang, Y. Q. Wang, H. C. Hu, X. N. Li, and L. J. Pan

Citation: Journal of Applied Physics **120**, 065103 (2016); doi: 10.1063/1.4960688
View online: http://dx.doi.org/10.1063/1.4960688
View Table of Contents: http://scitation.aip.org/content/aip/journal/jap/120/6?ver=pdfcov
Published by the AIP Publishing

Electric transport coefficients in highly epitaxial $LaBaCo_2O_{5+\delta}$ films with "p-to-n" transition induced by oxygen deficiency

J. Shaibo,[1] Q. Y. Zhang,[1,a)] Y. Q. Wang,[2] H. C. Hu,[1] X. N. Li,[1] and L. J. Pan[1]
[1]*Key Laboratory of Materials Modification by Laser, Ion and Electron Beams, and School of Physics and Opto-electronic Technology, Dalian University of Technology, Dalian 116024, People's Republic of China*
[2]*College of Physics, Qingdao University, Qingdao 266071, China*

(Received 5 June 2016; accepted 28 July 2016; published online 10 August 2016)

Electric transport coefficients such as carrier type, density, and mobility are the important physical parameters in designing functional devices. In this work, we report the study on the electric transport coefficients of the highly epitaxial $LaBaCo_2O_{5+\delta}$ (LBCO) films, which were discussed as a function of electric conductivity for the first time and compared with the results calculated by the theory for mixed conduction. The mobility in the LBCO films was determined to be ~0.85 and ~40 cm^2/V s for holes and electrons, respectively, and the density of *p*-type carriers strongly depends on the oxygen deficiency. Solid evidence is presented to demonstrate that the oxygen deficiency cannot make LBCO materials changed from *p*- to *n*-type. The *n*-type conduction observed in experiment is a counterfeit phenomenon caused by the deficiency in Hall measurement, rather than a realistic transition induced by oxygen deficiency. In addition, the temperature-dependent conductivity was discussed using the differential coefficients, which might be useful in the study of the samples with magnetic transition. *Published by AIP Publishing.*
[http://dx.doi.org/10.1063/1.4960688]

I. INTRODUCTION

$La_{0.5}Ba_{0.5}CoO_3$ (LBCO), which derives from $LaCoO_3$ by doping Ba ions at the *A* site in the ABO_3 perovskite, is one of the strongly correlated electron oxides. LBCO materials exhibit a wide range of electric, magnetic, and optical properties that are scientifically interesting and technologically important. LBCO materials are shared by three similar forms, namely, the ordered, the nano-scale ordered, and the disordered phases,[1] depending on the cationic ordering or disordering of Ba and La ions, thus exhibiting the diversity in physical properties. For instance, the ordered LBCO with space group *P4/mmm* is semiconducting, but the other two phases with space group $Pm\bar{3}m$ are semi-metallic.[1] Due to their catalytic activity, LBCO materials have been considered promising for surface catalyst and chemical sensor,[2] and the leading material as the cathode of solid oxide fuel cells operating at intermediate temperatures.[3–11] On the other hand, the materials also have potential for the applications of functional devices relevant to giant magnetoresistance (GMR) and spintronics. Recently, epitaxial *Ln*BCO films (*Ln* = lanthanoid) were successfully deposited on the substrates with cubic lattice, including MgO, $SrTiO_3$ (STO), $LaAlO_3$, and $NdGaO_3$, using a pulsed laser deposition (PLD) method,[12–20] paving the way for fabrication of functional devices. As a matter of fact, the sheet resistance was reported changing over 99% in a few seconds during switching between 4% H_2 + 96% N_2 and O_2,[12] and then highly sensitive gas sensors were demonstrated in reducing/oxidizing environments.[13,14]

For applications of functional devices, a basic work is to investigate the physical properties such as electric conductivity, ferromagnetism, and GMR. In addition, electric transport coefficients, such as carrier type, density, and mobility, are significant for fabrication of widely used components like metal-semiconductor contacts and *p-n* junctions, but such data are still unavailable in the literature for *Ln*BCO films. Furthermore, *Ln*BCO is one kind of materials extremely sensitive to oxygen deficiency, which is usually a factor uncontrollable in the film preparation. Therefore, it is necessary to study the influence of oxygen deficiency on the electric transport coefficients. On the other hand, *Ln*BCO are the materials with intrinsic *p*-type conduction, but *n*-type conduction is frequently observed in the Hall or Seebeck measurement.[21–27] The *p*-to-*n* transition was attributed to the formation of oxygen defects (or formation of Co^{2+}),[23] contamination of impurity elements,[21,26] and/or deviation from the stoichiometry of cationic compositions,[27] whereas the true reasons need further exploration. In this work, we report the study on the electronic transport properties of the highly epitaxial LBCO films on MgO substrates, using Hall measurement along with characterization of the films' microstructure. To reveal the nature of *p*-to-*n* transition induced by oxygen deficiency, the films were deposited at similar thicknesses and annealed in the atmospheres such as O_2, H_2, N_2, or Ar, separately, and then, the electric transport coefficients were systematically studied using the theory for mixed conduction.

II. EXPERIMENTAL DETAILS

The LBCO films were deposited on (001) MgO substrates in the size of 5 × 5 mm under the optimized conditions of 800 °C and 1×10^{-4} Pa by a PLD method, using Nd:YAG laser ($\lambda = 355$ nm, 10 Hz, and 58 mJ/pulse) focused on a ceramic LBCO target. The deposition was carried out for 2 h, producing a film thickness of ~200 nm. Before

a)Author to whom correspondence should be addressed: qyzhang@dlut.edu.cn

cooling down to room temperature (RT), the films were *in situ* annealed for 15 min at $\sim 1 \times 10^{-4}$ Pa. In order to minimize any non-uniformity, the as-grown films were first annealed at 900 °C for 3 h in a tube furnace with oxygen atmosphere prior to other annealing treatments, subsequently annealed at 350 °C for 30 min separately in pure H_2, Ar, or N_2 for producing oxygen deficiency in the films, and then slowly cooled down to RT. For convenience in description, the as-grown film was named as S0, and the samples annealed in O_2 were labeled as S-O. The samples undergoing another annealing process in N_2, Ar, or H_2 were labeled as S-N, S-Ar, and S-H, respectively. To study the recoverability of the electric conduction, one of the S-N samples was annealed again in O_2 at 900 °C for 3 h, thus was labeled as S-N/O. The LBCO films were characterized by a transmission electron microscopy (TEM, JEM-ARM200F) and high-resolution x-ray diffraction (XRD, Bruker D8 and Panalytical X'Per MRD). The electric transport coefficients, namely, carrier density, mobility, and conductivity, were measured at RT by the Swin Hall 8800 system with a magnetic field of 6100 Gauss. The resistance at the temperatures ranging from RT down to 10 K was measured using a four probe system via Agilent B2900A. The electrodes were made by the method similar to the report in the literature.[28]

III. RESULTS AND DISCUSSION

A. Microstructures of the LBCO films

XRD and TEM examination showed that all of the films are single-crystalline, with the epitaxial relationship of $[100]_{LBCO}//[100]_{MgO}$ and $(001)_{LBCO}//(001)_{MgO}$, as shown in Figs. 1(a) and 1(b), which were taken from the S-O and S-N samples, respectively. We can see that the annealing process did not lead to great damage to the films except for making a change in the lattice parameters, which could be deduced from the peak shifts in the XRD patterns, as shown in Fig. 2. It is known that the ordered LBCO phase has the symmetry with space group *P4/mmm* and the other two phases have the symmetry with space group $Pm\bar{3}m$. For the film samples, however, identifying the two microstructures by XRD and electron diffraction is impossible, because the atomic scattering factors of La^{3+} and Ba^{2+} ions are very close to each other in one hand. On the other hand, the tiny difference between the lattice parameters of *a* and *c*, corresponding to the in-plane and the out-plane lattice constants, respectively, is blurred out by the film strains imposed by the substrates. Therefore, we used the structure with cubic perovskite to index the XRD patterns of the LBCO films in this study. All the XRD peaks could be indexed by (00 *l*), illustrating the *c*-axes of the films oriented normal to their surfaces.

The XRD peak shifts revealed the out-plane lattice constants strongly dependent on the oxygen content in the films. For example, the XRD peaks of the sample annealed in O_2 were shifted to the high angle with respect to the as-grown film (S0), indicating that the oxygen incorporation into the film leads to a shorter *c*. When the sample was annealed in the ambient absent of oxygen, such as in N_2, Ar, or H_2, the *c* value was increased. The increase in the out-plane lattice parameter can be essentially ascribed to the enhancement in

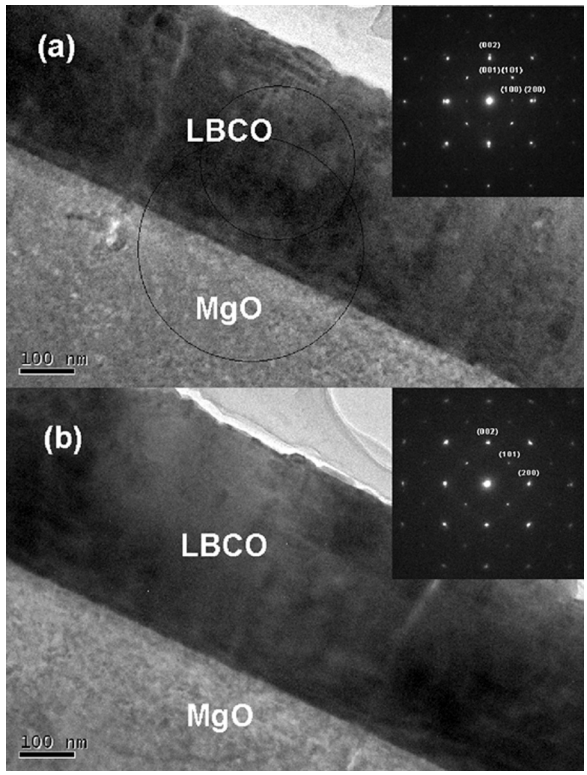

FIG. 1. Cross-sectional TEM photographs of the LBCO films annealed in O_2 (a) and N_2 (b). The insets are the selected area electron diffraction taken at the interfaces, as indicated in Fig. 1(a). The structure is indexed by cubic perovskite.

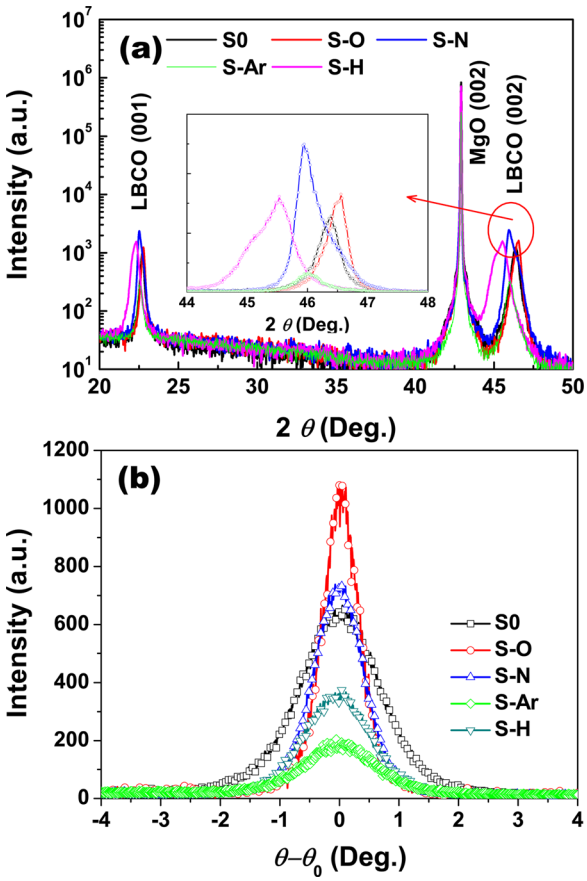

FIG. 2. X-ray diffraction patterns (a) and rocking curves of (002) diffraction (b) of the LBCO films annealed in O_2, N_2, Ar, and H_2 in comparison with the as-grown sample. The inset zooms in the (002) peaks of the LBCO films.

the Coulomb repulse between the cations due to the removal of O ions, in accordance with our previous study.[5] For the as-grown film, the full width at half maximum (FWHM) of (002) XRD rocking curve is as large as 1.57°. After annealing in O_2 at 900 °C for 3 h, the FWHM decreases to 0.72°, as shown in Fig. 2(b), indicating the improvement in crystallinity. However, the crystallinity went worse when the films underwent another annealing process in the ambient absent of oxygen, even at the temperature as low as 350 °C, suggesting that oxygen deficiency produced relatively large lattice strain.

The lattice parameters were further studied using the reciprocal space maps (RSMs) recorded at the (204) reflections of the LBCO films and the MgO substrates, as shown in Fig. 3. Using the RSMs, we calculated the lattice parameters and the expansion with respect to the unit cell of the LBCO bulk material with stoichiometry,[1] as listed in Table I. We found that the in-plane parameters of all films are similar ($\Delta a/a_0 = 1.0 \pm 0.2\%$) and a change is observed in the parameters normal to the film surfaces ($\Delta c/c_0 = 1.1\%$–4.4%). With consideration of the annealing processes, we have a conclusion that the lattice strain in the LBCO films is increasing with the increase in oxygen vacancies (V_O), and the volume of unit cell is indicative of the oxygen deficiency, which could be tailored from $\delta \approx 0.2$ to $\delta \approx 0.9$ in *Ln*BCO materials.[29] Therefore, we further deduce that the oxygen vacancies in the samples annealed in O_2 and H_2 are the lowest and the highest, respectively, and the samples annealed in N_2 and Ar have the similar V_O concentrations.

B. Electric transport coefficients

Room-temperature Hall measurement showed that the electric conductivity is highly sensitive to the oxygen contents in the films, changing from $\sim 1.4 \times 10^{-2}$ to $\sim 3.6 \times 10^{2}$ S/cm, more than 4 orders of magnitude. The as-grown films exhibit *p*-type conduction with a relatively low conductivity. After annealing in O_2 at 900 °C for 3 h, the *p*-type conduction is significantly improved due to the incorporation of oxygen in the films. These *p*-type films conformably changed to be "*n*-type" when they were annealed in the ambient absent of oxygen, as depicted in Table II. These "*n*-type" films could be recovered to be *p*-type after undergoing another annealing process in O_2, again demonstrating that the oxygen content controls the electric transport properties of LBCO films. Similar *p*-to-*n* transitions have been observed in Hall or Seebeck measurement of *Ln*BCO bulk materials and other perovskite oxides.[21–27] Usually, such a *p*-to-*n* transition was simply attributed to the formation of oxygen defects (or formation of Co^{2+}),[23] contamination of impurity elements,[21,26] and/or deviation from the stoichiometry of cationic composition.[27] However, *no one challenges to the validity of Hall measurement as well as Seebeck measurement*.

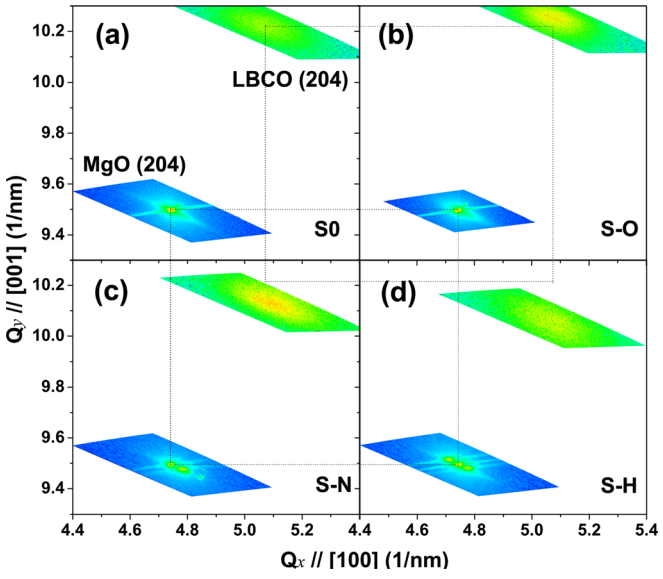

FIG. 3. Asymmetric RSMs at (204) diffraction of the LBCO films and the MgO substrates. The color in the RSMs represents the XRD intensity varying in logarithmic scale, and the maximum scales for LBCO (204) and MgO (204) are 10^2 and 10^7 in counts, respectively. The dotted squares indicate the deviation of S-O, S-N, and S-H with respect to S0.

TABLE I. Lattice parameters and expansion of the LBCO film samples with respect to the stoichiometric bulk materials ($a_0 = 0.38977$ and $c_0 = 0.77158$ nm (Ref. 1)).

Sample	a (nm)	c (nm)	$\Delta a/a_0$	$\Delta c/c_0$	$\Delta V/V_0$
S0	0.3946	0.7828	0.0124	0.0145	0.0398
S-O	0.3943	0.7802	0.0116	0.0112	0.0348
S-N	0.3928	0.7896	0.0078	0.0234	0.0393
S-Ar	0.3929	0.7886	0.0080	0.0220	0.0385
S-H	0.3946	0.8055	0.0124	0.0440	0.0700

As shown in Table II, there are many doubts in the "*n*-type" LBCO films determined by Hall measurement. (1) The density of free electrons in these "*n*-type" films is not reasonable if oxygen vacancies are the major donors. For instance, the density of free electrons in the S-Ar sample is much higher than that in the S-H sample, conflicting with the conclusion from the structural characterization. (2) It is rather abnormal that the mobility in some "*n*-type" samples is much smaller than that in *p*-type samples. It is well known that the mobility is a function of the effective mass of carriers[30] and the free electrons should have the mobility larger than that of holes. (3) It is not acceptable that the two as-grown samples as well as the two S-H samples undergoing the same annealing process have rather different electric transport coefficients. As a matter of fact, similar doubts are frequently observed in determination of the electric transport coefficients in other semiconducting films, but do not receive enough attention. When plotting the data in Table II as a function of electric conductivity, we found that the carrier density and mobility strongly depends on the electric conductivity, as indicated by the symbols in Fig. 4. The films with high conductivity are *p*-type. When the electric conductivity decreases to a low level, the films change to be "*n*-type". The abnormal electric transport coefficients, both the carrier density and the mobility, are only observed in the vicinity of $\sim 1 \times 10^{-1}$ Ω cm. As all of the films were deposited at a thickness of ~200 nm with good crystallinity, the reasons originating from the film quality and the thickness can be excluded. Therefore, we believed that the conductivity-dependent coefficients are related to the principle of Hall measurement.

TABLE II. Conductivity, carrier type, density, and mobility of various LBCO films determined by Hall measurement at room temperature.

Sample	Carrier type	Conductivity (S/cm)	Carrier density (cm^{-3})	Hall mobility (cm^2/V s)
S0-1	*p*	0.5096	4.31×10^{18}	0.7377
S0-2	*p*	0.1379	3.32×10^{20}	0.0026
S-O	*p*	14.94	1.10×10^{20}	0.8468
S-N/O	*p*	364.7	2.67×10^{21}	0.8512
S-H1	*n*	0.0137	-1.78×10^{18}	0.0481
S-H2	*n*	0.0784	-7.53×10^{17}	0.6494
S-Ar	*n*	0.0840	-1.80×10^{19}	0.0291
S-N	*n*	0.2082	-1.86×10^{18}	0.6993

For a semiconductor in thermal equilibrium, free electrons coexist with holes. In experiment, however, Hall or Seebeck coefficient is given by assuming that there is one kind of carriers. This assumption is valid only when the density of major carriers is sufficiently high. In an intrinsic semiconductor or an extrinsic semiconductor with heavy compensation, both electrons and holes can be participated in the conduction process; thus, the mixed conduction prevails in the carrier transport.[30] In this case, Hall coefficient is expressed by[30]

$$R_{\mathrm{H}} = \frac{n_p\mu_p^2 - n_n\mu_n^2}{e(n_p\mu_p + n_n\mu_n)^2}, \tag{1}$$

where n_n and n_p are the realistic densities of electrons and holes, respectively, and μ_n and μ_p are the corresponding mobilities. If $R_{\mathrm{H}} > 0$, the sample will commonly be assigned to be *p*-type. Conversely, if $R_{\mathrm{H}} < 0$, the sample is *n*-type. The apparent carrier density, which is measured in experiment, is calculated by Hall coefficient, or

$$n = \left|\frac{1}{R_{\mathrm{H}}e}\right| = \left|\frac{(n_p\mu_p + n_n\mu_n)^2}{n_p\mu_p^2 - n_n\mu_n^2}\right|. \tag{2}$$

The apparent Hall mobility is given by

$$\mu_{\mathrm{H}} = |R_{\mathrm{H}}\sigma| = \left|\frac{n_p\mu_p^2 - n_n\mu_n^2}{n_p\mu_p + n_n\mu_n}\right|, \tag{3}$$

where σ is the conductivity. It is clear that the apparent carrier density and the mobility are close to the realistic values for the samples with $n_p\mu_p^2 \gg n_n\mu_n^2$ or $n_p\mu_p^2 \ll n_n\mu_n^2$. For a sample with $n_p\mu_p^2 \approx n_n\mu_n^2$, however, the apparent carrier density will go to extremely high, up to infinite, with the apparent mobility approaching to zero. This conclusion is highly in accordance with our observation in experiment. Therefore, we concluded that the electric transport coefficients directly measured from the samples with low conductivity are not realistic.

In principle, Hall measurement cannot determine the realistic electric transport coefficients in the case of $n_p\mu_p^2 \approx n_n\mu_n^2$. To give a reasonable estimation of these coefficients in the LBCO films, we calculated the apparent Hall mobility (μ^{App}) and the carrier density (n^{App}) as a function of the electric conductivity, and compared them with the experimental data, as shown in Fig. 4, in which the sharp peaks correspond to the critical point ($n_p\mu_p^2 = n_n\mu_n^2$) for apparent "*p*-to-*n*" transition in the films. The calculations were carried out under the assumption that the mobilities of free electrons and holes are constants in these samples, because all the LBCO films exhibited the single-crystal feature with good crystallinity. In our calculations, we used $\mu_p = 0.85\ \mathrm{cm}^2/\mathrm{V\ s}$, which is the value determined in the *p*-type films with a hole density sufficiently high, and $\mu_n = 40\ \mathrm{cm}^2/\mathrm{V\ s}$, which was estimated from a H-annealed LBCO film on STO substrate. We found that the calculated μ^{App} and n^{App}, as well as the apparent conduction type determined in experiment, highly in conformity with most of the experimental data when the density of free electrons was set to $n_{\mathrm{n}} = 3.5 \times 10^{14}\ \mathrm{cm}^{-3}$ (the thick

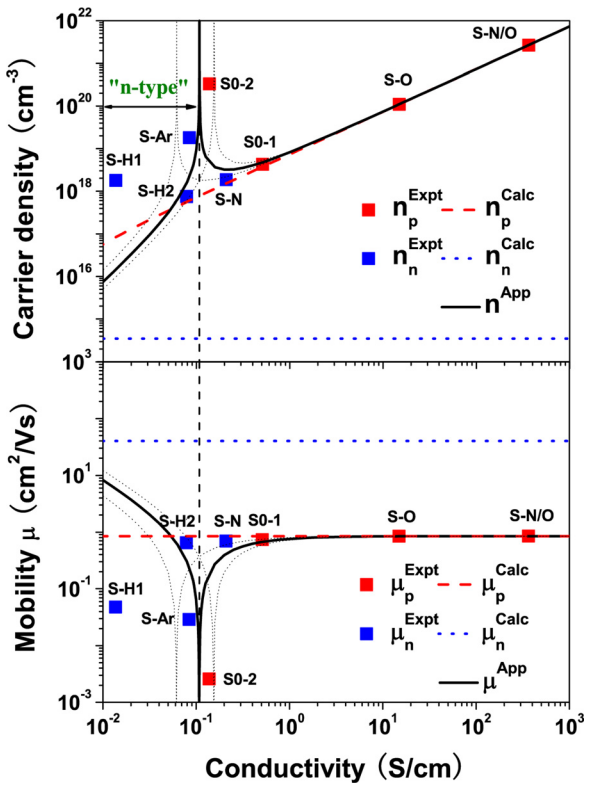

FIG. 4. Electric transport coefficients plotted as functions of conductivity, in which the solid squares are the experimental data listed in Table II, and the curves are calculated by the theory for mixed conduction. The calculations were carried out under assumption of $\mu_n \sim 40\ \mathrm{cm}^2/\mathrm{V\ s}$, and $\mu_p = 0.85\ \mathrm{cm}^2/\mathrm{V\ s}$ by setting $n_{\mathrm{n}} = 3.5 \times 10^{14}\ \mathrm{cm}^{-3}$ (the thick solid lines) and $n_{\mathrm{n}} = 2.0 \times 10^{14}$ or $n_{\mathrm{n}} = 5.0 \times 10^{14}\ \mathrm{cm}^{-3}$ (the thin dotted lines), respectively. The vertical thick dashed line is plotted at the critical point for the apparent *p*-to-*n* transition in Hall measurement.

solid lines in Fig. 4). If setting $n_n = 2.0 \times 10^{14}$ cm^{-3} or $n_n = 5.0 \times 10^{14}$ cm^{-3} (the two thin dotted lines in Fig. 4), an obvious discrepancy between the calculated curves and experimental data could be observed, indicating that the critical point for the apparent "*p*-to-*n*" transition is very sensitive to the density of free electrons, and a small deviation in the density of free electrons will produce a quite large change in μ^{App} and n^{App} in the vicinity of the critical point. Therefore, we are convinced that the calculated carrier density (n_p^{Calc} and n_n^{Calc}) and the mobility (μ_p^{Calc} and μ_n^{Calc}) are closer to the realistic values in these samples, rather than the data directly determined in experiment.

As shown in Fig. 4, the calculated density and mobility of holes (n_p^{Calc} and μ_p^{Calc}) in the *p*-type samples with high conductivity are very close to that determined by Hall experiment (n_p^{Expt} and μ_p^{Expt}), because holes are dominant in these samples. For the *p*-type samples in vicinity of $n_p\mu_p^2 \approx n_n\mu_n^2$, $n^{App} \approx n_p^{Expt} \gg n_p^{Calc}$, and the discrepancy between n_p^{Calc} and n^{App} or n_p^{Expt} could be as large as several orders of magnitude. For example, n_p^{Expt} is more than two orders of magnitude larger than n_p^{Calc} in one of the as-grown samples, leading to $\mu_p^{Expt} \ll \mu_p^{Calc}$. After correction by the mixed-conduction theory, the densities of holes in the two as-grown samples are similar, thus more acceptable than the results directly determined in experiment. As for the "*n*-type" samples, our calculations showed that the realistic density of holes is 2–3 orders of magnitude higher than that of free electrons, though Hall coefficients are negative due to $n_p\mu_p^2 < n_n\mu_n^2$. Therefore, the *p*-type conduction ($\sigma_p = en_p\mu_p$) in these "*n*-type" samples is still dominant, larger than 97.5% in the total conductivity. Based on our calculations, we have a confident conclusion that oxygen deficiency cannot make a *p*-to-*n* transition for the LBCO films, at least at room temperature, even for the samples with the large amount of oxygen vacancies.

The good agreement between the theoretical and the experimental results reveals an important fact that the density of free electrons in these films is relatively low, and maintains at a level approximately constant in the LBCO films with different oxygen contents. This conclusion excludes the possibility of oxygen vacancies as donors in LBCO materials, because the difference in oxygen deficiency is rather large in these films. Though oxygen vacancies make few contributions to the density of free electrons, oxygen deficiency is a crucial factor controlling the density of holes in the LBCO films, probably by changing the valences of Co ions. For instance, removal of O ions from the lattices leads to a change from Co^{3+} to Co^{2+} and reduces the density of holes in the materials. As shown in Fig. 4, the as-grown films usually exhibit *p*-type conduction, but the density of holes is relatively low ($\sim 10^{18}$ cm^{-3}), which can be attributed to the large amount of oxygen vacancies in the samples. After annealing in O_2, reduction in oxygen vacancies produced an obvious increase in the density of holes, up to 2.67×10^{21} cm^{-3}. For the samples undergoing another annealing process in the ambient absence of oxygen, the electric conductivity was decreased to a level lower than that of the as-grown samples because more oxygen vacancies were created, and then the apparent "*n*-type" conduction was detected in the Hall experiment. The "*n*-type" conduction is a counterfeit phenomenon induced by both the relatively high mobility of free electrons and the low density of holes, rather than originating from the increase in the density of free electrons. As a matter of fact, the nearly constant density of free electrons in the LBCO films is an indication that the free electrons originate primarily from the thermal excitation of electrons from the valence band to the conduction band, and/or the impurity donors, but cannot be ascribed to oxygen vacancies. This conclusion is of significance for fabrication of LBCO-based devices. More importantly, the conductivity-dependent plot is a practical method to determine the realistic electric transport coefficients in intrinsic semiconductor or extrinsic semiconductor with heavy compensation.

C. Temperature-dependent conductivities

To further explore the electric transport properties of the LBCO films, the electric conductivities were measured as a function of temperature, as shown Fig. 5(a), in which the temperature-dependent conductivity of the ordered LBCO bulk material with stoichiometry was plotted after the work of Rautama *et al.*[1] for comparison. With respect to the LBCO bulk material, the films exhibit much lower conductivities, which can be essentially ascribed to the decrease in the density of holes induced by oxygen deficiency. On the other hand, the film thickness is at a level of ~200 nm, as shown in Fig. 1; thus, the scattering of carriers by the surface and interface[31] is considerably enhanced, leading to the increase in the film resistivity, especially at low temperatures. Though the electric conductivities of the films change as large as 4 orders

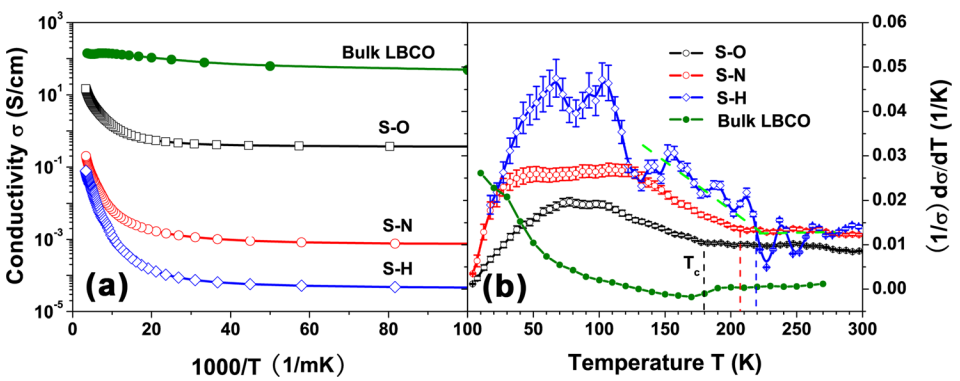

FIG. 5. (a) Conductivities and (b) their differential coefficients ($\frac{1}{\sigma}\frac{d\sigma}{dT}$) plotted as a function of temperature for the LBCO films annealed in O_2, N_2, and H_2. The data of LBCO bulk material with stoichiometry after the work of Rautama *et al.*[1]

of magnitude with the increase in oxygen deficiency, their temperature dependence suggests that these films could be regarded as heavy-doping semiconductors.

For heavy-doping semiconductors, we cannot use the temperature-dependent conductivity to determine the physical parameters related to the materials, such as the activation energy of carriers, mainly due to two heavy-doping effects.[30] The first consideration is that the Fermi-Dirac statistics must be employed to calculate the carrier density, instead of using the Boltzmann statistics. The second heavy-doping effect is related to the band gap narrowing. The two heavy-doping effects obstruct us deeply discussing the physical parameters related to the materials because of the absence of adequate theory. However, we found that the temperature-dependent conductivity could be further discussed using its differential coefficient ($\frac{1}{\sigma}\frac{d\sigma}{dT}$), which provides us the massages relevant to the magnetic transition in the LBCO films, as shown in Fig. 5(b). Despite the difference in the differential coefficients between the LBCO films and the bulk material, we could take a transition temperature below room temperature in these samples. For the sample annealed in O_2, the transition takes place at a temperature of $T_c \sim 180$ K, very close to the Curie temperature of ferromagnetic transition observed in the highly epitaxial LBCO films ($\sim$170 K)[16,18] or in the LBCO bulk material ($\sim$178 K).[1] A similar change in resistivity has ever been reported in the *Ln*BCO bulk materials with metal-insulator (MI) transition, such as $GdBaCo_2O_{5+\delta}$ and $HoBaCo_2O_{5+\delta}$,[32] but is rarely observed in the materials without MI transition. Therefore, we have a deduction that the magnetic transition in the materials might lead to a change in conductivity due to the variation in spin scattering.[33] For the samples annealed in N_2 and H_2, the transition temperatures are at $\sim$208 and $\sim$220 K, suggesting that oxygen deficiency seems to result in the increase in transition temperature, but this phenomenon needs a deep exploration along with magnetic measurement.

We found the value of $\frac{1}{\sigma}\frac{d\sigma}{dT}$ is strongly dependent on the oxygen deficiency in the sample. To give a confident conclusion, the differential coefficient was discussed using the theory of semiconductors. In a semiconductor, the differential coefficient of conductivity can be expressed by

$$\frac{1}{\sigma}\frac{d\sigma}{dT} = \frac{1}{\sigma}\frac{d\sigma_p}{dT} + \frac{1}{\sigma}\frac{d\sigma_n}{dT}. \tag{4}$$

When *p*-type conduction is dominant ($\sigma \approx \sigma_p = n_p \mu_p e$) and the mobility slowly varies with temperatures, which is true for most of semiconductors, we have

$$\frac{1}{\sigma}\frac{d\sigma}{dT} \approx \frac{1}{n_p}\frac{dn_p}{dT} + \frac{1}{n_n}\frac{dn_n}{dT}\frac{\mu_n n_n}{\mu_p n_p}. \tag{5}$$

As $\frac{1}{n_p}\frac{dn_p}{dT} \approx \frac{1}{n_n}\frac{dn_n}{dT}$ and $\frac{\mu_n}{\mu_p}$ is approximately constant, Eq. (5) reveals a fact that the density ratio of free electrons to holes (n_n/n_p) plays a crucial role in determining the differential coefficient. At a given temperature, the density of free electrons determined by thermal excitation maintains at an approximate constant in all of the samples; thus, the ratio of n_n/n_p varies with the density of holes in the samples. In the LBCO films, the density of holes is a function of V_O concentration; thus, the value of $\frac{1}{\sigma}\frac{d\sigma}{dT}$ is increasing with the increase in oxygen deficiency. This conclusion is highly in accordance with our observation that $\frac{1}{\sigma}\frac{d\sigma}{dT}$ in the sample with a high conductivity is smaller than that in the sample with a low conductivity. More importantly, our results demonstrate that the differential coefficient of conductivity or resistivity might be a useful tool to study the electric transport in the materials with magnetic transition.

IV. CONCLUSIONS

The electric transport coefficients of highly epitaxial LBCO films with oxygen deficiency were studied using Hall measurement and discussed for the first time using the theory for mixed conduction. The quantitative calculations demonstrated that oxygen vacancies unlikely act as donors contributing to the *n*-type conduction; thus, oxygen deficiency cannot make LBCO materials changed from *p*- to *n*-type. The observed *p*-to-*n* transition induced by oxygen deficiency is essentially ascribed to the deficiency in the principle of Hall measurement, rather than a realistic transition. At a given temperature, the density of holes in the highly epitaxial LBCO films depends strongly on the oxygen content, maintaining the density of free electrons approximately constant in the samples with different oxygen contents. The LBCO films with oxygen deficiency exhibited the electric transport properties close to heavy-doping semiconductor, with a room-temperature mobility of $\sim$0.85 and $\sim$40 cm^2/V s for holes and electrons, respectively. Our results reveal a fact that electric conductivity is an important factor that should be considered in analyzing transport coefficients of semiconductors. In addition, the differential coefficients were found highly sensitive to the variation in the temperature-dependent conductivity and thus are useful for investigating the influence of magnetic transition on the electric transport properties.

ACKNOWLEDGMENTS

The authors acknowledge Professor W. Y. Ding in Dalian Jiaotong University for his help in Hall measurement and Dr. M. Liu in Xi'an Jiaotong University for his help in characterization of microstructures. One of the authors, J. Shaibo, would like to thank the support from Chinese Government Scholarship (Grant No. 2012736005). Professor L. J. Pan is thankful to his financial support from the National Natural Science Foundation of China under Grant No. 11274055.

[1]E. L. Rautama, P. Boullay, A. K. Kundu, V. Caignaert, V. Pralong, M. Karppinen, and B. Raveau, Chem. Mater. **20**, 2742 (2008).
[2]M. L. Post, J. J. Tunney, D. Yang, X. Du, and D. L. Singleton, Sens. Actuators, B **59**, 190 (1999).
[3]M. Daturi, G. Busca, and R. J. Willey, Chem. Mater. **7**, 2115 (1995).
[4]S. L. Pang, X. N. Jiang, X. N. Li, Q. Wang, and Q. Y. Zhang, Mater. Chem. Phys. **131**, 642 (2012).
[5]S. L. Pang, X. N. Jiang, X. N. Li, H. X. Xu, L. Jiang, Q. L. Xu, Y. C. Shi, and Q. Y. Zhang, J. Power Sources **240**, 54 (2013).
[6]T. Kawada, K. Masuda, J. Suzuki, A. Kaimai, K. Kawamura, Y. Nigara, J. Mizusaki, H. Yugami, H. Arashi, N. Sakai, and H. Yakogawa, Solid State Ionics **121**, 271 (1999).

[7]T. Inagaki, K. Miura, H. Yoshida, R. Maric, S. Ohara, X. Zhang, K. Mukai, and T. Fukui, J. Power Sources **86**, 347 (2000).
[8]T. Ishihara, S. Fukui, and H. Nishiguchi, Solid State Ionics **152–153**, 609 (2002).
[9]K. Zhang, L. Ge, R. Ran, Z. P. Shao, and S. M. Liu, Acta Mater. **56**, 4876 (2008).
[10]C. Setevich, L. Mogni, A. Caneiro, and F. Prado, J. Electrochem. Soc. **159**, B73 (2012).
[11]D. Garcés, C. F. Setevich, A. Caneiro, G. J. Cuello, and L. Mogni, J. Appl. Cryst. **47**, 325 (2014).
[12]J. Liu, G. Collins, M. Liu, C. L. Chen, J. C. Jiang, E. I. Meletis, Q. Y. Zhang, and C. Dong, Appl. Phys. Lett. **97**, 094101 (2010).
[13]S. Y. Bao, C. R. Ma, G. Chen, X. Xu, E. Enriquez, C. L. Chen, Y. M. Zhang, J. L. Bettis, M.-H. Whangbo, C. Dong, and Q. Y. Zhang, Sci. Rep. **4**, 04726 (2014).
[14]M. Liu, S. P. Ren, R. Y. Zhang, Z. Y. Xue, C. R. Ma, M. L. Yin, X. Xu, S. Y. Bao, and C. L. Chen, Sci. Rep. **5**, 10784 (2015).
[15]M. Liu, J. Liu, G. Collins, C. R. Ma, C. L. Chen, J. He, J. C. Jiang, E. I. Meletis, A. J. Jacobson, and Q. Y. Zhang, Appl. Phys. Lett. **96**, 132106 (2010).
[16]M. Liu, C. R. Ma, J. Liu, G. Collins, C. L. Chen, J. He, J. C. Jiang, E. I. Meletis, L. Sun, A. J. Jacobson, and M.-H. Whangbo, ACS Appl. Mater. Interfaces **4**, 5524 (2012).
[17]C. R. Ma, M. Liu, G. Collins, H. B. Wang, S. Y. Bao, X. Xu, E. Enriquez, C. L. Chen, Y. Lin, and M.-H. Whangbo, ACS Appl. Mater. Interfaces **5**, 451 (2013).
[18]C. R. Ma, M. Liu, J. Liu, G. Collins, Y. M. Zhang, H. B. Wang, C. L. Chen, Y. Lin, J. He, J. C. Jiang, E. I. Meletis, and A. J. Jacobson, ACS Appl. Mater. Interfaces **6**, 2540 (2014).
[19]Q. Zou, M. Liu, G. Q. Wang, H. L. Lu, T. Z. Yang, H. M. Guo, C. R. Ma, X. Xu, M. H. Zhang, J. C. Jiang, E. I. Meletis, Y. Lin, H. J. Gao, and C. L. Chen, ACS Appl. Mater. Interfaces **6**, 6704 (2014).
[20]M. Liu, Q. Zou, C. R. Ma, G. Collins, S. B. Mi, C. L. Jia, H. M. Guo, H. J. Gao, and C. L. Chen, ACS Appl. Mater. Interfaces **6**, 8526 (2014).
[21]A. Maignan, D. Flahaut, and S. Hébert, Eur. Phys. J. B **39**, 145 (2004).
[22]A. A. Taskin, A. N. Lavrov, and Y. Ando, Phys. Rev. **71**, 134414 (2005).
[23]K. Berggold, M. Kriener, C. Zobel, A. Reichl, M. Reuther, R. Müller, A. Freimuth, and T. Lorenz, Phys. Rev. B **72**, 155116 (2005).
[24]K. Iwasaki, T. Ito, T. Nagasaki, Y. Arita, M. Yoshino, and T. Matsui, J. Solid State Chem. **181**, 3145 (2008).
[25]H. Kozuka, H. Yamada, T. Hishida, K. Yamagiwa, K. Ohbayashi, and K. Koumoto, J. Mater. Chem. **22**, 20217 (2012).
[26]S. R. Sehlin, H. U. Anderson, and D. M. Sparlin, Phys. Rev. B **52**, 11681 (1995).
[27]J. Mizusaki, T. Sasamoto, W. R. Cannon, and H. K. Bowen, J. Am. Ceram. Soc. **65**, 363 (1982).
[28]J. Liu, M. Liu, G. Collins, C. L. Chen, X. N. Jiang, W. Q. Gong, A. J. Jacobson, J. He, J. C. Jiang, and E. I. Meletis, Chem. Mater. **22**, 799 (2010).
[29]C. Frontera, A. Caneiro, A. E. Carrillo, J. Oró-Solé, and J. L. García-Muñoz, Chem. Mater. **17**, 5439 (2005).
[30]S. S. Li, *Semiconductor Physical Electronics*, 2nd ed. (Springer Science, 2006).
[31]A. F. Mayadas, J. Appl. Phys. **39**, 4241 (1968).
[32]A. Maignan, C. Martin, D. Pelloquin, N. Nguyen, and B. Raveau, J. Solid State Chem. **142**, 247 (1999).
[33]F. Fauth, E. Suard, and V. Caignaert, Phys. Rev. B **65**, 060401 (2001).